MRS Advances

Making Soft Optical Sensors More Wearable

Cindy Harnett

University of Louisville J.B. Speed School of Engineering, 2210 S Brook St, Louisville, KY 40208, U.S.A

ABSTRACT

This paper discusses new components and approaches to make stretchable optical fiber sensors better meet the power and washability requirements of wearables. First, an all-polymer quick connector allows the light source and photosensor to be quickly detached for washing. Second, the paper investigates the possibility of driving the sensors using ambient light instead of an onboard light source. While optical strain sensors and touch sensors have advantages over electronic ones in wet environments, and the intrinsic stretchability of the fibers is useful for soft robotics and highly conformal wearables, the typical light-emitting diode (LED) light source consumes more power than an electronic resistive or capacitive strain sensor. In this work, ambient light of uniform but unknown intensity is demonstrated to drive an elastomeric optical touch sensor in a differential configuration.

INTRODUCTION

Elastomeric optical fibers are a new low-cost, all-polymer sensor material for measuring human activity in textile-borne and wearable formats. Researchers have recently demonstrated coating [1], molding [2], and extrusion-based [3] methods for making stretchable optical fibers. These fibers have a high refractive index core and low refractive index cladding. They transmit less light when stretched thanks to the increased length of the optical path, which includes total internal reflection events at the core-cladding interface (Fig. 1). The resulting optical loss coefficient α (dB/cm) is a function of core-cladding interface smoothness as well as each material's intrinsic optical absorbance.

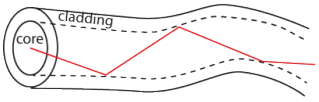

Figure 1: Optical fiber construction.

Threadlike fibers constructed as in Fig.1 can be applied to fabrics by sewing or adhesives, and cast waveguides can be bonded to finished garments. After their light intensity signals are transformed into electronic signals using optoelectronic sensors, the activity data can be

sent over a wireless link for analysis. However, for wearables, practical requirements must be taken into account.

The rest of this manuscript deals with two approaches to improving wearability: a quick connector and an investigation of ambient light as a signal source. The quick connector is briefly introduced in this section, while ambient light sensing is investigated in more detail throughout the rest of the paper.

Quick Connector

Wearables with integrated electronics, such as resistive strain sensors and conductive-fiber electrodes for sensing the electrical activity of skeletal muscles (electromyography or EMG) commonly transmit analog signals to a data acquisition and communication circuit using a metal snap fastener. This reversible connector lets the user detach the relatively expensive communication module from the EMG sticker so the sticker can be disposed, or from the resistive textile so the textile can be washed. Fabric-integrated optical fibers need a quick-connect equivalent of the snap fastener. Figure 2 shows a 3D printable housing that temporarily attaches the fiber to a notched printed circuit board (PCB) containing a photosensor or light source.

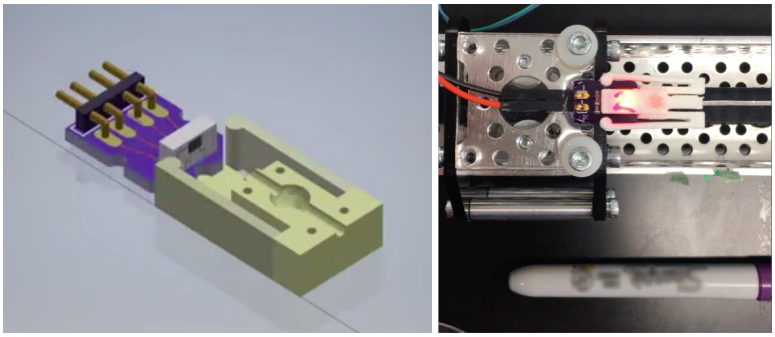

Figure 2: 3D printed quick connectors to align stretchable optical fibers with optoelectronic sources and detectors. Left: illustration with photosensor board, right: LED connector in a stretching experiment. Marker at lower right is 1 cm wide for scale.

Squeezing the sides of the connector detaches it from the PCB. Because the fiber diameter will decrease as it undergoes strain, the fiber will slip out of a cylindrical clamp (such as heat shrink tubing) if there is no adhesive or mechanical anchor. In the illustration of Figure 2, the housing has a bowl-like indentation that is filled with silicone adhesive to form an anchor on the fiber. This part is covered by a cap in the photo.

Ambient Light Driven Sensing

Another limitation of fiber-based optical sensors is their power consumption compared to electronic sensors. While they are still practical for battery-powered wearable systems, the light emitting diode (LED)-driven optical fiber strain sensors consume significantly

more power (~10 mW) than do resistive strain sensors made from conductive fibers (~0.1 mW). For both types of sensor, the receiving electronics—whether a photodiode or amplifier, draw far less power than even a low-power LED. The LED is turned off when not in use, but peak power requirements of optical sensors may still prevent their use in lightweight, battery-free energy-harvesting wearables.

Classifying and quantifying ambient light

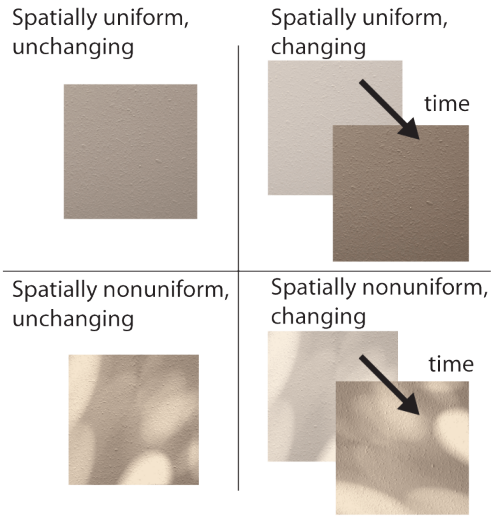

Figure 3: Classifications for ambient light.

Ambient light is available at no power cost, but at unknown intensity. Furthermore, its spatial distribution can be non-uniform, it can vary over time (Fig. 3) and its spectrum is unknown. While the spectrum at the receiver can be controlled with passive filters, the intensity and uniformity variations shown in Figure 3 will generally require a reference sensor. The light level in homes, offices, and other daily environments is usually described in *lux*, an intensity unit weighted according to the spectral response of the human eye [4]. Typical lux values are 50 lux for hallways, 300 for reading lamps, 1000-2000 for detailed task lighting, and 5000 for an overcast sky outdoors.

Differential sensor concepts for ambient light driven sensing

Figure 4 shows how elastomeric waveguides might be used in various strain sensing and touch location sensing modes. A reference signal is necessary to make sense of the data when the ambient light intensity is unknown. The method in this paper obtains a reference signal through differential absorption in a mismatched waveguide pair. Differential sensing, a highly effective method for canceling out temperature or strain effects in conventional electronics, is making inroads into soft electronics [5] as a way to isolate the signal of interest from the background. In this manuscript, we adjust the material's optical transmission with

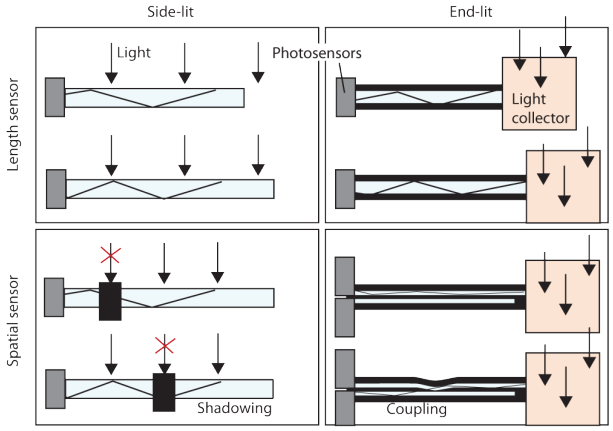

Figure 4: Designs for length and touch sensing in side-lit (left) and end-lit (right) formats.

additives and can then compare the signal intensity from two parallel fibers with known optical transmission differences, cancelling out the unknown ambient light intensity.

At the left side of Figure 4 are *side-lit* waveguides where ambient light enters the fiber cladding and a fraction of the light is guided toward the photodetector. These designs are useful for uniform/unchanging and uniform/changing light conditions (top row of Fig. 3) but not for spatially varying light. The *end-lit* designs on the right side of Fig. 4 use a light collector, for instance, a diffusing material connected to the fiber end. Because the light collector performs a spatial average, it might be able to handle the more challenging non-uniform lighting conditions in the bottom row of Fig. 3. In the rest of this paper, the focus is on the shadow-based side-lit touch sensor concept in the lower left of Fig. 4.

THEORY

In the lower left of Fig. 4, a portion of the incoming ambient light is blocked from entering the cladding by a finger or a stylus. The lux reading at Sensor A is then:

$$A = I\int_0^{x-s/2} e^{-\alpha_1 x'}dx' + I\int_{x+s/2}^{L} e^{-\alpha_1 x'}dx' \tag{1}$$

where I is the unknown ambient intensity scattered toward the detector (per unit length of waveguide), x is the location of the stylus center, s is the stylus width, α_i is the loss coefficient of waveguide A, and L is the waveguide length. If another sensor B is constructed from a material having a different loss coefficient α_2, the normalized differential intensity is:

$$\frac{A-B}{A} = \frac{I\int_0^{x-s/2} e^{-\alpha_1 x'}dx' + I\int_{x+s/2}^{L} e^{-\alpha_1 x'}dx' - I\int_0^{x-s/2} e^{-\alpha_2 x'}dx' - I\int_{x+s/2}^{L} e^{-\alpha_2 x'}dx'}{I\int_0^{x-s/2} e^{-\alpha_1 x'}dx' + I\int_{x+s/2}^{L} e^{-\alpha_1 x'}dx'} \tag{2}$$

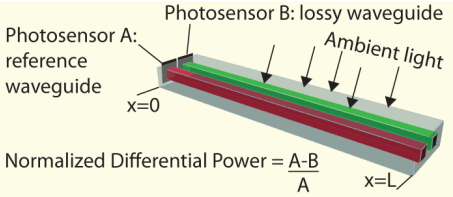

Figure 5: Differential waveguide setup.

This setup is illustrated in Figure 5. Here, the unknown ambient intensity I cancels out, but thanks to the different loss coefficients, the normalized differential intensity is not constant but is a function of the stylus position x. This equation assumes a uniform spatial intensity and direction, but its amplitude need not be known and it can vary over time.

EXPERIMENT

In previous work, process-based methods were used to modify the light attenuation coefficient of fibers [6]. In this work, however, 2 mg of a pigment (Silc-Pig black pigment, Smooth-On, Inc.) was mixed with 10 g of a liquid-cure silicone (Solaris, Smooth-On, Inc.) to reduce its optical transmission. Figure 5 shows the waveguide construction. Two 1x1mm square waveguides, 8 cm long with a 4 mm center-to-center separation, were cast in a laser-cut acrylic mold, one with the pigmented Solaris and one

with unmodified Solaris. The waveguides were clad with Solaris that had been mixed with 20 wt % Dow Corning 705 silicone oil. During the Solaris curing process, the oil formed an emulsion and did not crosslink. The oil droplets were then removed after curing by soaking the structure 12 hours in chloroform, followed by 8 hours in acetone. The resulting microscopic air pockets produced a low density elastomeric cladding that permitted waveguiding but also allowed light to enter the waveguides from the side. The completed waveguides were each connected to a separate VEML7700 ambient light sensor (Vishay, Inc) for data collection under different uniform lighting intensities from a desk lamp. Intensity readings were collected to compute normalized differential power (A-B)/A as a black cardboard shadow (Figure 6, left) was moved to different positions along the fiber pair.

RESULTS

The plot in Figure 6 shows the normalized differential power for both 900 lux and 1600 lux fall on the same line to within measurement error, regardless of the light intensity. The fit is from Equation (2).

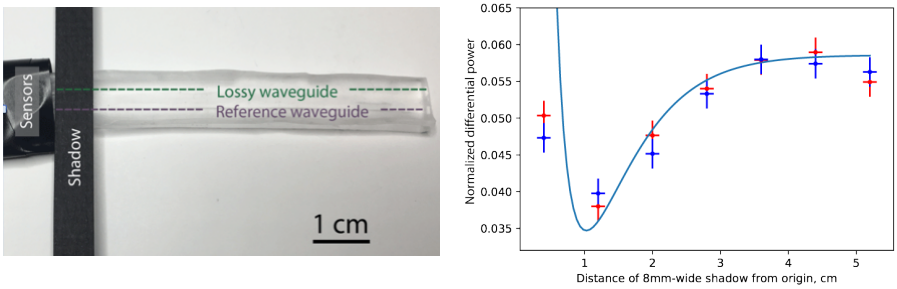

Figure 6: Left, image of waveguide pair and 8 mm wide "stylus." Right: normalized differential power under 900 lux (blue) and 1600 lux (red) uniform lighting as a function of stylus position.

DISCUSSION

While the differential sensor concept was successful at cancelling out the unknown incident light intensity, the plot in Figure 6 is not monotonic. The steep, negatively sloped section near zero is the most sensitive region, yet with these materials the sensitive region is only 1 cm wide; with the current materials almost no measurable light can reach the sensors from greater than 3 cm from the origin. Development of waveguides and materials with greater optical transmission would expand this region toward the size of human hands and touchscreens. Putting a low-loss elastomer (0.05 dB/cm) as the reference sensor and a more attenuating, but still low-loss material as the lossy sensor (0.2 dB/cm) into Equation 2 can be shown to expand the sensitive region out to 10 cm. Since out of the four application cases in Figure 4, the shadowing sensor is the only one that does not require the waveguides to be deformable, it should also be possible to implement this sensor in glass or another highly transmissive material. Light collection materials are already of great interest for solar energy applications; their development would enable other types of ambient-light driven strain and touch sensors illustrated in Fig. 3.

CONCLUSIONS

This manuscript demonstrated some improvements toward making soft optical sensors compatible with wearable systems: a quick-connect component, a classification of ambient light and the applicability of different sensing approaches to drive optical strain sensors with ambient light, and a proof-of-concept demonstration of an ambient light-driven touch sensor. If sufficient external light is available to make measurements, the light source can be turned off, cutting out the main power-consuming component in an optical sensor system and reducing its power consumption to the resistive sensor level. Unlike resistive sensors, no signal return path is required for fibers that use ambient light, making for a simpler device layout. Since textiles increasingly form the skins of soft robots in addition to wearables, new developments here will lead to sensorized surfaces in a wide range of applications.

ACKNOWLEDGMENTS

Partial support was received from NSF award 1849213. Thanks to the Spring 2019 University of Louisville ECE Capstone student lab team (Oliver de Boer, Kurtis Dotson and Logan Schaufler) for producing the illustration in Fig. 2.

REFERENCES

[1] C. K. Harnett, H. Zhao, and R. F. Shepherd, Adv. Mat. Tech. 2, 1700087 (2017).
[2] J. Guo, X.Liu, N. Jiang, A. K. Yetisen, H. Yuk, C. Yang, A. Khademhosseini, X. Zhao, and S.-H. Yun, Adv. Mat. **28** (46), 10244-10249 (2016).
[3] A. Leber, B. Cholst, J. Sandt, N. Vogel, and M. Kolle, Adv. Funct. Mat. **29** (5), 1802629 (2019).
[4] J. J. Vos, Color Research and Application **3** (3), 125-128 (1978).
[5] K. L. Dorsey, M. Cao, and G. A. Slipher, IEEE Sens. J. **18** (18), 7505–7512 (2018).
[6] M. Campbell, P. Singh, K. Kate, and C. K. Harnett, MRS Advances **4** (23), 1341–1347 (2019).